Detection of Sensitization and Intergranular Corrosion of Fe-Cr-Ni Alloys

Vivekanand Kain, R.C. Prasad* and P.K. De

Metallurgy Division, Bhabha Atomic Research Centre
Trombay, Mumbai 400 085, India
**Metallurgy & Materials Science Dept., Indian Institute of Technology, Mumbai 400 076, India*

1. INTRODUCTION

Stainless steels (SSs) and Fe or Ni base super-alloys are commonly used in industrial applications requiring a good combination of mechanical strength, formability and corrosion resistance /1,2/. Among the family of Fe-Cr-Ni alloys, austenitic SSs are the work horses, with applications ranging from cryogenic (such as liquification of gases) to high temperatures (such as superheaters in power plants). SSs owe their excellent corrosion resistance to the protective 'passive' film formed over the surfaces. This thin, tenacious and self-healing oxide film forms on surfaces of alloys containing more than 12% chromium. However, as is the case with other materials with passive films, SSs are prone to localised forms of corrosion viz crevice, pitting, intergranular corrosion (IGC) and stress corrosion cracking (SCC). Austenitic stainless steels when exposed to the temperature range 475-850°C become susceptible to IGC in particular environments. Other varieties of stainless steels (ferritic and duplex SSs) also undergo IGC. Among other Fe-Cr-Ni alloys, Inconel 600 and Incoloy 800 are particularly susceptible to IGC. In fact, all those Fe-Ni-Cr alloys which initially contain more than 12 percent chromium are prone to IGC /3/. Upon exposure to the temperature range 475-850°C, chromium and carbon react at grain boundaries to form chromium-rich carbides. This temperature range may be encountered during isothermal heat treatments, slow cooling from higher temperatures (e.g., solution annealing or during shutdown of plants operating at high temperatures), elevated temperature service or during welding. Irrespective of the reason for exposure to the said temperature range, the process of precipitation of chromium carbide is called 'sensitization'. The chromium-rich carbide is $M_{23}C_6$ in the case of austenitic and ferritic stainless steels /4/ and $M_{23}C_6$ and M_7C_3 in the case of nickel-base alloys and martenitic and duplex stainless steels /5/. In fact, under certain conditions, even annealed Fe-Cr-Ni alloys have been reported to have undergone IGC.

IGC is a localised attack at and adjacent to the grain boundaries with relatively little corrosion of the grains. It manifests as disintegration (falling out of grains) and loss of strength. The technological and economic impact of this particular mode of corrosion is immense. The stainless steels and nickel-base alloys are used in speciality industries requiring excellent corrosion resistance. Loss of mechanical or physical integrity is of major consequence in such plants, and safety aspects also have to be considered, as it may lead to loss of corrosive/radioactive liquids. A survey of corrosion failures /6/ in metallic piping and equipment by a chemical company in the early 70s showed that IGC accounts for about 11% of total corrosion failures, SCC for about 26% and pitting for about 16%. It should be noted that in certain plants handling corrosive process fluids, e.g. nitric acid, sulfuric acids, etc., IGC is of prime concern and other forms of corrosion may not manifest at all. In addition, the causative factors for IGC also promote intergranular SCC and pitting corrosion in many cases. Therefore, the phenomenon which makes SSs and nickel-base alloys prone to IGC is of the utmost concern. Various aspects of this, e.g. the mechanism of IGC, assessment (testing) procedures and recent advances in these procedures, are covered in this paper. The work carried out in the Metallurgy Division of BARC in these areas is described to illustrate developments in understanding the basic

mechanism and the basis in assessing the susceptibility to IGC.

2. MECHANISM

To explain the absence of any significant attack on the grain matrix and the preferential attack at and along the grain boundaries that occurs in the case of IGC, four main theories have been put forward. Detailed discussions on these theories are presented in many articles /1,3,7/ and they are briefly summarized here:

2.1. The Noble Carbide Theory

It has been postulated that IGC is an electrochemical reaction between the 'noble' carbide particles and the 'active' adjacent matrix, and proceeds along grain boundaries when there is a continuous path provided by connected carbides. However, in oxidizing environments the grain matrix adjacent to the carbides should also be 'passive' and should not cause IGC. Also, the observation of IGC resistance of Fe-Cr-Ni alloys containing carbides but no depletion zones cannot be explained by this theory.

2.2. The Stress Theory

The proponents of this theory assumed that considerable local stresses appear in zones where the second phase begins to precipitate and grow gradually. Even development of potential differentials due to differences in the energy of steel structures was predicted. However, it was later argued that the boiling solutions (for testing) would relieve these small stresses and the thermal stresses developed during heat treatments would be much larger than stresses developed due to precipitation.

2.3. The Chromium Depletion Theory

This theory, first proposed by Bain *et al.* /4/, describes precipitation of $Cr_{23}C_6$ at the grain boundaries (when exposed to the temperature range 475 - 850°C) and development of Cr depletion zones adjacent to the carbides. When the Cr level in the depletion zone goes below about 12%, the passive film formed on the Cr depletion zones becomes weak and breaks easily when exposed to corrosive solutions. These Cr-depleted regions then undergo fast attack because of (a) galvanic contact and (b) an unfavourable area ratio. However, IGC of annealed materials not containing the carbides/ depleted regions cannot be explained by this theory.

2.4. The Segregation Theory

It was shown that segregation of solutes (e.g. P, S and Si) at grain boundaries also renders the Fe-Cr-Ni alloys susceptible to IGC in highly oxidizing environments, e.g. nitric acid-containing hexavalent Cr ions.

A large number of studies on the IGC behaviour of Fe-Cr-Ni have been reported in the literature since the advent of the above-mentioned theories. It has become clear that the chromium depletion theory is able to explain most cases of IGC. Direct observations of the depletion of Cr in the regions adjacent to the carbides have been made and the profiles of Cr depletion have also been measured by TEM studies /8-10/. It has been observed that the minimum level of chromium may go to 5-15% in the depleted regions of Fe-Cr-Ni alloys /9/. However, to explain observations of IGC in alloys not containing carbides, the segregation theory holds good. It may be mentioned that such observations are restricted to highly oxidising environments. The observations of IGC in alloys containing secondary (Cr-rich) phases, other than $Cr_{23}C_6$, is also well documented /6/. Intergranular attack on heat-treated duplex stainless steels containing a Cr-rich sigma phase at grain boundaries has been demonstrated even when the sigma phase is submicroscopic. This occurs for Fe-Cr-Ni alloys containing Mo and/or high levels of Cr. The final possibilities leading to IGC are shown schematically in Fig. 1.

3. EFFECT OF ALLOYING ELEMENTS

Sensitization, the causative factor for IGC, develops due to precipitation of $Cr_{23}C_6$. Therefore both the Cr and carbon content of Fe-Cr-Ni alloys play an important role /1,7/. Usually these alloys contain carbon in excess of the solubility limit. The higher the amount of carbon in excess of the solubility limit of carbon in the matrix, the greater is the tendency for sensitization. This is the reason for sensitization of ferritic SSs con-

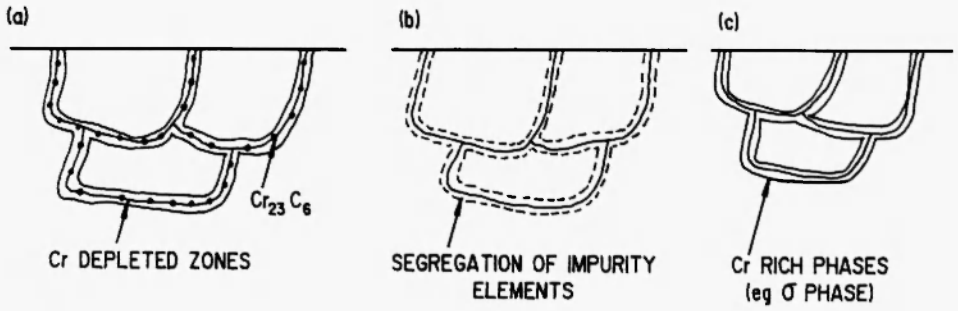

Fig. 1: Three conditions of Fe-Cr-Ni alloys rendering them susceptible to intergranular corrosion: (a) formation of Cr depletion zones, (b) segregation of impurity elements, and (c) precipitation of Cr-rich phases.

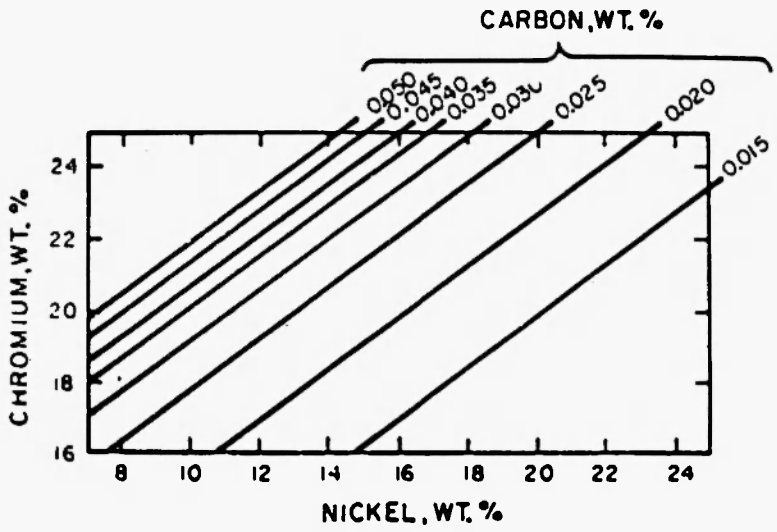

Fig. 2: Effect of chromium and nickel content on the carbon content required to avoid intergranular attack on stainless steels in the strauss test after sensitization at 650°C for one hour /11/.

taining only 0.01 - 0.02% carbon, as the solubility limit in the ferritic matrix is very low. On the other hand, austenitic SSs require more than 0.03% carbon for IGC to occur. Similarly, for alloys with higher chromium levels, more precipitation would be required to achieve depletion of chromium to levels less than 12%. Chromium is also reported to increase the solubility of carbon in the matrix, making less carbon available for the reaction forming $Cr_{23}C_6$. The effect of Mo is to decrease the susceptibility to IGC. It is suggested that Mo forms Mo_2C at grain boundaries, preventing carbon from reacting with chromium. Also, the main role of Mo is to increase the activity of Cr in the Cr-depleted zones causing retardation of the growth of carbide /10/. Molybdenum increases passivity on the surfaces, hence Mo-bearing alloys require extended depletion to render them prone to IGC. Nickel, on the other hand, reduces the solubility of carbon in the matrix, making available more and more carbon for carbide precipitation /11/. A balance must be struck between Cr, Ni and C in the alloys to avoid sensitization. Cihal *et al.* /11/ showed this relationship in Fig. 2.

Another minor alloying addition, nitrogen, improves the sensitization resistance if present in an amount of up to 0.16% in austenitic stainless steels /12/. It has been reported that it retards sensitization by increasing Cr levels in the depletion zones, thereby retarding the growth of carbides. Above about 0.16%, precipitation of Cr_2N itself causes Cr depletion zones /12/.

4. ASSESSMENT OF SUSCEPTIBILITY TO IGC

The susceptibility to IGC in Fe-Cr-Ni alloys is assessed by some standard ASTM tests, as well as the Electrochemical Potentiodynamic Reactivation (EPR) and other NDT tests. A brief description of these is given below:

4.1. ASTM Standard Tests

These test procedures (A 262) involve the microstructure development of alloys in the practice A. The 'step' or 'dual' structures are taken as resistant to IGC whereas in the case of a 'ditch' structure, some other practice (B-F) has to be resorted to, depending upon the end use of the material. Except for practice A, all other practices are (a) destructive, (b) time consuming and (c) qualitative in nature. The other specified tests in ASTM, to evaluate the susceptibility of high alloy steels, including nickel-base alloys, are the G-28 tests. The operating details of A 262 and G-28 tests are listed in Table 1 along with generally used acceptance criteria for various alloys. The critical assessment of ASTM A 262 tests, the acceptance criteria generally used and quantification procedures have been covered in many review articles /13,14/.

4.2. EPR Tests

The fact that the Cr depletion zones with less than 12-13% Cr would not develop a strong passive film and would subsequently be attacked in corrosive solutions is

Table 1
Parameters of various standard tests of ASTM used to evaluate susceptibility to IGC of various Fe-Cr-Ni alloys

Test name	Solution composition	Test procedure	Assessment criterion	Acceptance criterion
A 262, ASTM				
Practice A	10% oxalic acid at room temperature	anodically etch at $1A/cm^2$ for 90 sec.	microstructure classification	step, dual - accept, ditch - test by other practices
Practice B	50 wt% H_2SO_4 + 25 g/litre $Fe_2(SO_4)_3$	120 hour exposure to boiling solution	weight loss per unit area	Type 304 SS (as received) Type 304L (677°C, 1 hr) < 48 mpy
Practice C	65 wt% HNO_3	Five 48 h exposures to boiling solution, refreshed after each test	average weight loss per unit area of five periods	Type 304/304L (as received) < 18 mpy Type 304:L (677°C, 1 hr) < 24 mpy
Practice D	10% HNO_3 + 3% HF	2, 2h exposures to 70° solution	comparison of ratio of weight loss of as received and lab-annealed samples of the same material	Ratio < 1.5
Practice E	16 wt% H_2SO_4 + 100 g/litre (6 wt%) $CuSO_4$ + metalalic copper	24-72 h exposure to boiling solution	appearance of cracks upon bending, or reduction in tensile properties	No cracks upon bending
Practice F	50 wt% H_2SO_4 + 100 g/litre $CuSO_4$	24-120 h exposure to boiling solution	appearance of cracks upon bending, weight loss per unit area	No cracks upon bending
G-28, ASTM				
Method A	50 wt% H_2SO_4 + 25 g/litre $Fe_2(SO_4)_3$	24-120 h exposure to boiling solution	weight loss per unit area	–
Method B	23% H_2SO_4 + 1.2% HCl + 1% $FeCl_3$ + 1% $CuCl_2$	24 h exposure to boiling solution	weight loss per unit area	–

made use of in electrochemical reactivation tests /15,16/. There are two versions of EPR tests, which are used to detect quantitatively the degree of sensitization. The advantages of these tests are that (a) they are very fast tests, (b) they are non-destructive in nature and can be used in the field, and (c) they are quantitative. The two versions of the test for type 304/304L SSs are described below:

4.2.1. Single-loop EPR test

The surface to be tested /17/ is immersed in a deaerated solution of 0.5 M H_2SO_4 + 0.01M KSCN at 30°C. The surface finish of the specimen surface should be 1 μm or better. A potential of +200 mV (SCE) is applied for 2 minutes and then the potential is reversed back at a scan rate of 6 V/h. This is shown schematically in Fig. 3a. The charge (Q) accumulated during the reactivation scan is measured by a current integrator. The P_a value is calculated by dividing it by the grain boundary area (GBA), as

$$GBA = A_s [5.09544 \times 10^{-3} \exp (0.34696X)] \quad (1)$$

where A_s is the sample area (cm^2), X is the ASTM grain size number measured at a magnification of 100. In this calculation of GBA, it is assumed that (a) the width of attack on sensitized material is always 2 (5×10^{-5}) cm, the width measured on nickel-base alloys /18/, (b) the attack is distributed uniformly over the entire grain boundary area and (c) the grains are round (spherical) in shape.

4.2.2. Double-loop EPR test

This method of testing /19,20/ does not require the fine surface finish of 1 μm. A surface finish with 120 grit emery paper is sufficient; however, more reproducible results could be obtained with a finer surface finish. The solution and temperature used are the same as for the single-loop version. However, in this version, the potential is scanned from the open circuit potential (OCP) value. This is shown schematically in Fig. 3b. The parameters measured in the test are the P_a value, i_r/i_a (i.e. peak reactivation current/peak activation current) and C_r/C_a (i.e. peak reactivation charge/peak activation charge). In calculating GBA, the assumptions are the same as those described in the single-loop method.

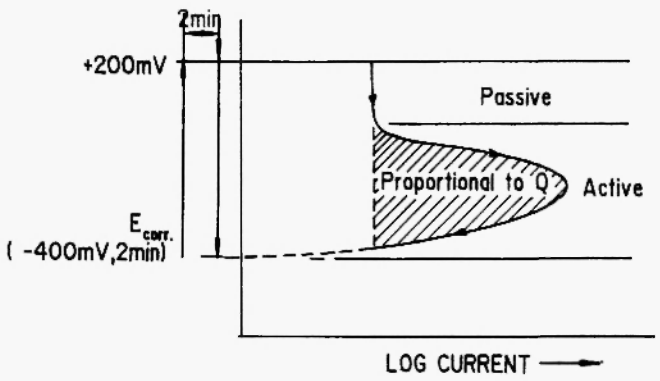

(a)

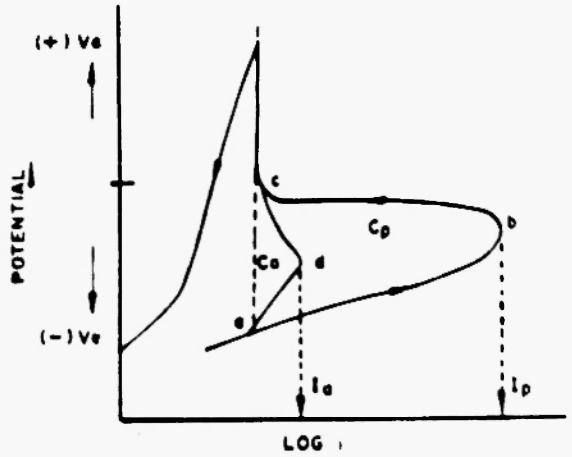

C_p – Passivation charge (area under a b c)
C_a – Reactivation charge (area under a d c)
I_a – Maximum current density reactivation
I_p – Maximum current density-passivation

$$P_a = \frac{C_a}{GBA} \text{ c/cm}^2$$

$GBA\ (cm^2) = A_s [5.09544 \times 10^{-3} \exp. (0.34696\ X)]$

X = ASTM grain size at 100 magnification.
A_s = Specimen area.

(b)

Fig. 3: Schematic diagram of EPR (a) single-loop and (b) double-loop methods for AISI 304/304L stainless steel /17,29/.

4.2.3. EPR for other Fe-Cr-Ni alloys

Minor variations of the parameters used in the EPR test for type 304/304L are used for testing other alloys.

The basic principles remain the same. Table 2 lists the operating parameters for type 316/316L, duplex SS, Inconel 600 and Incoloy 800.

4.2.4. Acceptance criteria

The P_a values, as measured by the EPR tests, have not been in common use to correlate to IGC behaviour. This is because the P_a values saturate for materials with high degrees of sensitization (i.e. ditch structures), but are very sensitive for materials with 'step' or 'dual' structure /17,20/. However, materials with 'step' or 'dual' structures are not prone to IGC and therefore such a correlation is not required. Studies correlating the P_a, i_r/i_a parameters with the results of practice B, A 262, ASTM showed that, for low degrees of sensitization, practice B is not very sensitive but is able to distinguish between two materials with high degrees of sensitization. Therefore, the two techniques – the EPR test and practice B, A 262, ASTM – are useful in different regions of sensitization regimes. However, Cihal /21/ using 2M H_2SO_4 (70°C), vertex potential (the maximum passivation potential) of 500 mV, double-loop mode and a scan rate of 15 V/h has given the criteria for acceptance of steels as follows: $C_aC_p \times 100$: <18 indicates no corrosion, 18-22 indicates trace corrosion, 28-37 indicates weak corrosion and >37 indicates strong corrosion.

In the case of Inconel 600, the correspondence between the EPR test, ASTM G28 test and STEM studies is better and it is also possible to detect the onset of desensitization /22/. For duplex SS or cast varieties of austenitic stainless steels, good correlations have been reported between i_r/i_a and corrosion rates obtained from modified strauss tests /23/.

4.3. Other Test Methods

Other electrochemical and non-destructive test methods have also been used to evaluate the susceptibility of Fe-Cr-Ni alloys to IGC/SCC. These are described here:

4.3.1. Constant potential etching

For high alloy SSs, such as type 254 SMO, 904 L and 18-13-3L (i.e. 18 Cr, 13 Ni, 3 Mo and low-carbon grade) SSs, constant potential etching (CPE) in 3M $HClO_4$ + xM HCl solution at room temperature has been reported /24/ to be more sensitive than the modified strauss test in evaluating their susceptibility to IGC. A constant potential of 0 mV (SCE) was used in solutions containing 1.5 M, 0.75 M and 0.50 M HCl for the three alloys, respectively, for a period of 10 to 15 min. The microstructure developed was evaluated under an optical microscope and the fraction of grain boundaries 'ditched' was evaluated. The results of these

Table 2
Operating parameters of the EPR tests for various Fe-Cr-Ni alloys

Material/ Parameter	AISI 316/316L	Duplex SS	Inconel 600		Incoloy 800
		Double-loop /22/	Single-loop /21/	Double-loop /23/	/21/
Electrolyte	0.5M H_2SO_4 + 0.01M KSCN	0.5M H_2SO_4 + 0.02M KSCN	1M H_2SO_4 + 0.001M KSCN	0.01M H_2SO_4 + 10 ppm KSCN	0.5M H_2SO_4 + 0.001M KSCN
Deaeration	Ar	Ar	N_2/Ar	N_2/Ar	N_2
Temperature (°C)	30°	25°	30°	25°	30°
Cathodic pre-treatment mV (SCE)	-600	–	-400	-400	-400
Vertex potential mV (SCE)	+200	+450	1160	600	400
Scan rate (mV/min)	100	50	180	30	200
Parameters for assessment	P_a, i_r/i_a, C_r/C_a	i_r/i_a	P_a	i_r/i_a	– – – –

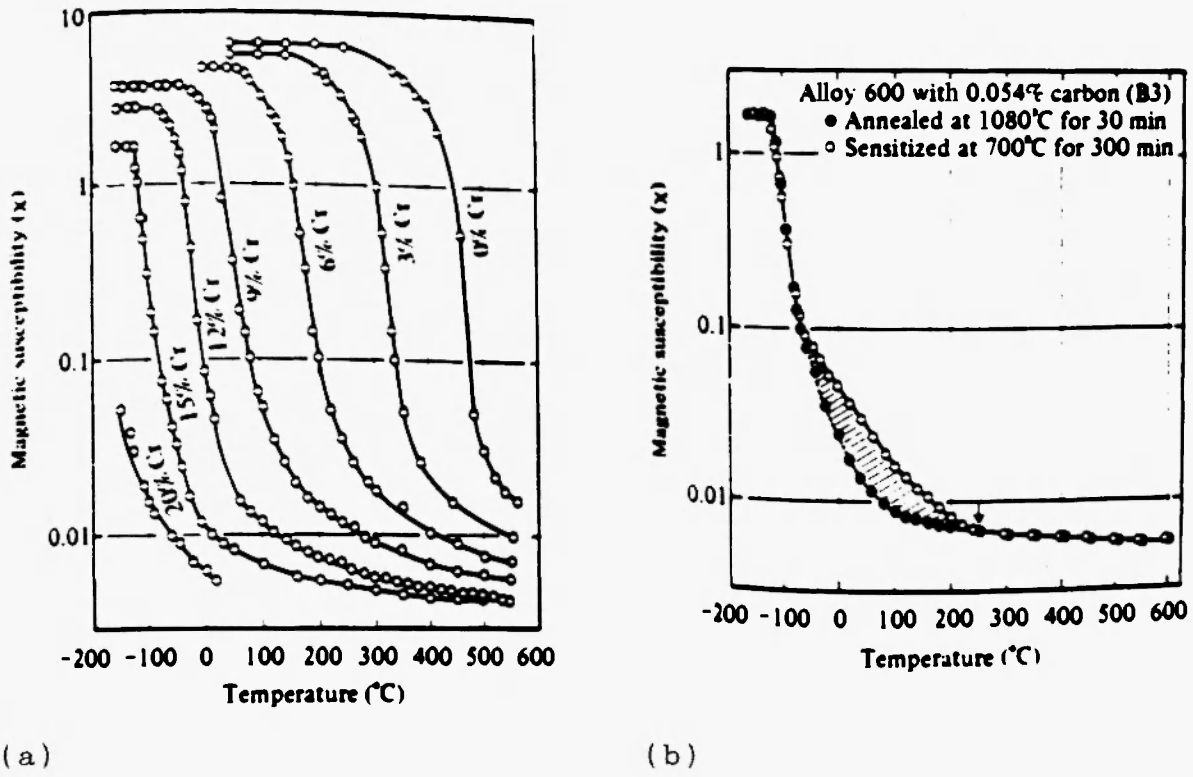

Fig. 4: (a) Change in curie points in nickel-base Cr-10Fe alloys, and (b) Magnetic susceptibility change as a function of measuring temperature in alloy 600 /25/.

tests compared well with the results of the modified strauss test, where the depth of attack after the strauss test was measured. It was shown that for low to medium levels of sensitization, the CPE test was more sensitive.

4.3.2. Non-destructive tests

The most successful method of detection of sensitization in Fe-Cr-Ni alloys has been the one based on magnetic susceptibility of the material. This method has been applied to Inconel (alloy) 600, where it has been shown that the magnetic susceptibility of chromium-depleted zones at grain boundaries was 100 to 1000 times larger than that of the matrix. This is shown in Fig. 4. Using a magnetic balance, Kowaka *et al.* /25/ measured magnetic susceptibility as a function of measuring temperature, clearly making a distinction between a sensitized and solution-annealed alloy, as shown in Fig. 4. Sensitized Alloy 600 with 0.054% carbon showed increased magnetic susceptibility at temperatures below 250°C, compared to solution-annealed alloy. This also allows determination of the minimum level of Cr in the depletion zones (Fig. 4a), and in their material, Kowaka *et al.* concluded that the chromium content in a sensitized alloy had dropped to a concentration of about 3%, from the 16% Cr in the matrix. Similar studies /26/ are also reported on Alloy 800.

However, for stainless steels, NDT techniques have not been found to be useful in the detection of sensitization. Eddy current, ultrasonic /27/ and electrical resistance testing /28/ have been found to be insensitive to detection of sensitization in the SSs. It has been reported /27/ that, after the exposure of sensitized SSs to corrosive environments, the extent of corrosion (or depth of penetration) can be measured using Eddy current testing.

5. EFFECT OF MATERIAL VARIABLES ON EPR TESTS

The test procedures and their results described earlier were for 'clean' materials affected only by sensitization, i.e. precipitation, of $Cr_{23}C_6$ and creation of Cr-depletion zones adjacent to the grain boundaries. The effect of parameters other than sensitization on the results of EPR tests is described below.

5.1. Effect of Prior Cold Work

Studies were carried out /29/ on type 304 SS, cold-worked in the range 10-55%. These samples were sensitized and their susceptibility to IGC was evaluated by the modified strauss test (i.e. measurement of percent reduction in ultimate tensile strength after exposure to practice E, A 262, ASTM). It was found that the susceptibility to IGC is maximum for the sample given about 20% cold work. The double-loop EPR test was also carried out on the cold-worked and sensitized sample and the results in terms of P_a, i_r/i_a and C_r/C_a are shown in Fig. 5 /29/. It is evident that the C_r/C_a is a parameter that correlates well with the results of modified strauss tests. The other two parameters, namely i_r/i_a and P_a, do not show good correlation because the current density for passivation (i_p) gets considerably altered by cold work in a 0.5M H_2SO_4 solution. Similarly, alteration of i_r is also affected by cold work, thus affecting both P_a and i_r/i_a values.

Therefore, use of the parameter C_r/C_a should be made to assess the degree of sensitization of stainless steels with prior cold work, so as to obtain a better correlation with the results of the strauss test.

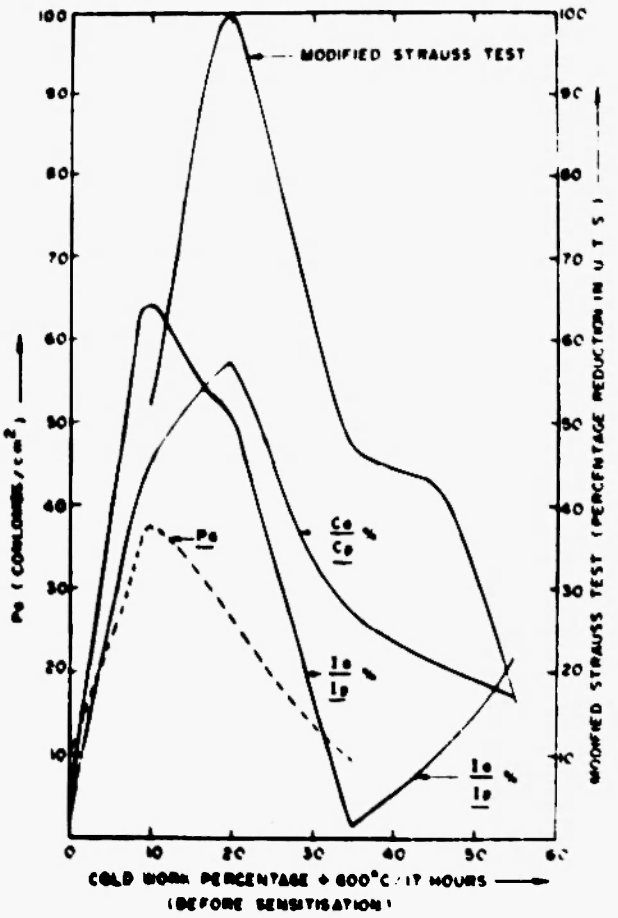

Fig. 5: Comparison of the EPR parameters with the modified strauss test results for cold-worked type 304SS /29/.

5.2. Effect of Active Inclusions

It has been reported /30/ that the presence of thin elongated stringers of sulphides or oxysulfides (of Fe and Mn) renders the SSs prone to end grain corrosion in oxidizing environments. A type 304 L SS with dual structure and containing these inclusions showed accelerated IGC due to corrosion initiated from end faces, in practice C of A 262, ASTM. The single-loop EPR test carried out on the cross-sectional and longitudinal surfaces of this material showed the effect of the inclusions very clearly. As the inclusions come under attack from the end faces (cross-sectional regions), the reactivation (P_a) is higher on the cross-sectional faces than on the longitudinal faces. The re-activation curves for (a) a material showing 'step' structure + inclusions and (b) a material with 'dual' structure + inclusions in both directions are shown in Fig. 6 /30/. Also shown in the figure are their micro-structures. This indicates that the single-loop EPR test is sensitive to the presence of 'active' inclusions. It has been reported /30/ that the double-loop version of the EPR test (P_a) can not distinguish between a material with inclusions and another without inclusions. This is attributed to etching out of inclusions in the forward

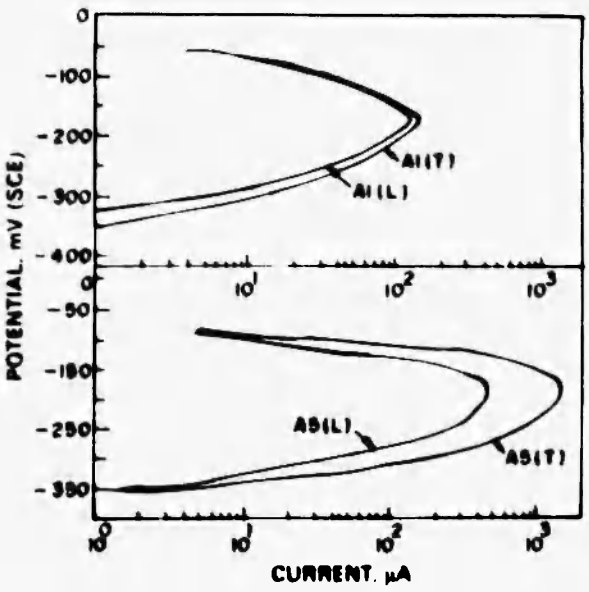

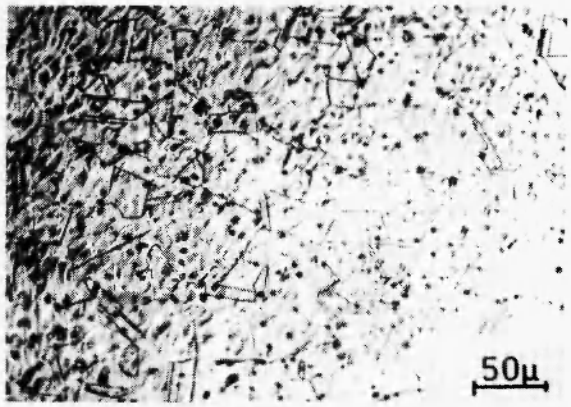

A1 transverse

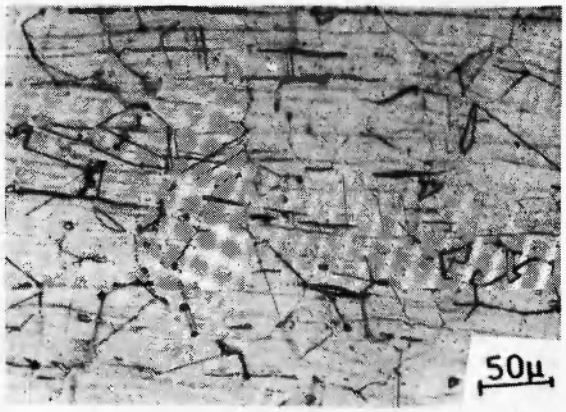

A1 longitudinal

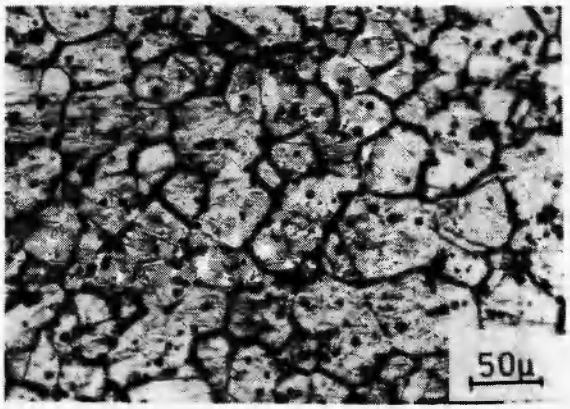

A5 transverse

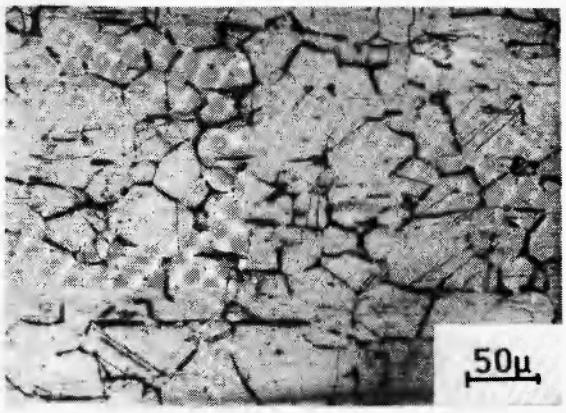

A5 longitudinal

Fig. 6: Effect of inclusions in transverse (T) and longitudinal (L) sections on reactivation loop of EPR test for type 304SS. Sample area of A1 = 0.185 cm^2 and A5 = 0.265 cm^2, and their respective microstructures /30/.

scan itself. Still, one should expect the i_r/i_a or C_r/C_a values to reflect the presence of inclusions. However, such studies are not reported.

5.3. Effect of Desensitization

It has been shown that a longer duration of heat treatments at sensitization temperatures causes replenishment of Cr depletion zones and results in densensitization /31/. A desensitized material contains a network of carbides at grain boundaries, but the Cr depletion zone adjacent to these is not present. This was shown by restoration of corrosion rates in practice C, A 262, ASTM for type 304 SS. The heat treatments at 750°C and 800°C caused severe sensitization (after one day and 30 min. heat treatment, respectively) and resulted in high corrosion rates in practice C. A 262, ASTM. However, the corrosion rates came down to levels similar to that observed for the solution-annealed sample after complete desensitization (after fifteen days and one day of heat treatment, respectively). This is reflected in the P_a values after the single-loop EPR test carried out on these samples and is shown in Fig. 7 /31/. It may be mentioned that a sensitized and desensitized sample appear similar after practice A, A 262, ASTM, both showing 'ditch' structure. However, the

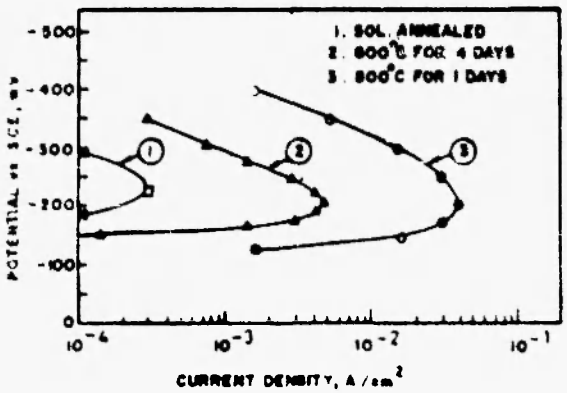

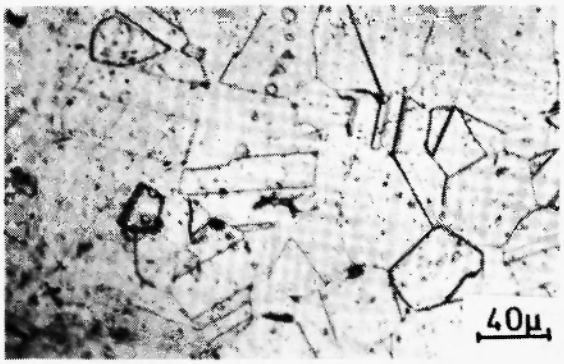

Solution annealed

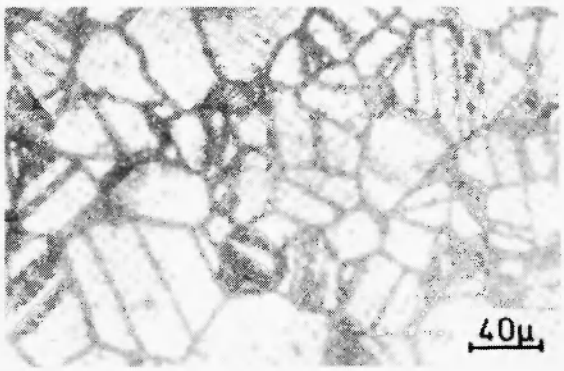

800°C, 4 days

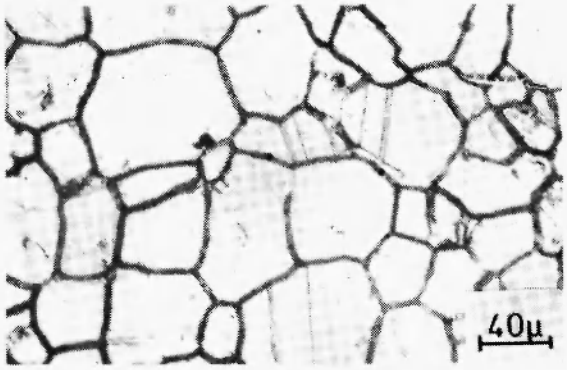

800°C, 1 day

Fig. 7: Reactivation curves for differently heat-treated 304 SS samples at 800°C and their respective microstructures /31/.

sensitized sample, which also contains Cr-depleted regions, shows a very high P_a value in the EPR test, and the desensitized sample, containing only carbides, shows low P_a values, similar to that obtained for the solution-annealed sample. This also indicates that the carbides in the sample are not attacked during the EPR test.

6. RECENT DEVELOPMENTS IN EPR TESTING

The round robin tests on EPR had shown good agreement between the results of both the versions of EPR tests performed at different laboratories /32/. This indicates that the specified surface preparation and testing procedure do not result in any variations in the final results. However, some new findings emerged from these round robin tests relating to (a) test temperature, (b) measurement of ASTM grain size and definition of reactivation area, and (c) effect of EPR on 'width' and 'depth' of Cr depletion regions. These and other aspects are described below to understand the basic mechanism involved in the EPR testing.

6.1. Test Temperature

EPR tests are strongly dependent on the testing temperature. Compilation of EPR results at the temperatures 10, 20, 30 and 40°C showed that the dissolution (reactivation) charge increases with increasing temperature of testing. Using these plots of ln Q/GBL and test temperature, and Arrhenius equation, an activation energy of dissolution of test material was calculated to be 67 ± 9 KJ/mole. The effects of testing temperatures and Arrhenius type plots are shown in Figs. 8 and 9 /32/, respectively. It was suggested that the test temperature basically affects the dissolution kinetics (hence dissolution charge), and it should be possible to convert the P_a value obtained at any temperature to the P_a value at 30°C, using the equation

$$P'_a = P_a \exp.\ \{26.55(30-T)/(273+T)\} \qquad (2)$$

where T is in °C.

6.2. Definition of Reactivation Area

The basic assumption in the EPR test is that all the grain boundaries contribute to the reactivation charge. This becomes true only when all the grain boundaries are sensitized (fully covered with depletion zones). However, for 'step' and 'dual' structures, it is never true. The second assumption was that the width of attacked grain boundaries was $2(5 \times 10^{-5})$ cm, which was taken from measurement of attacked grain boundaries

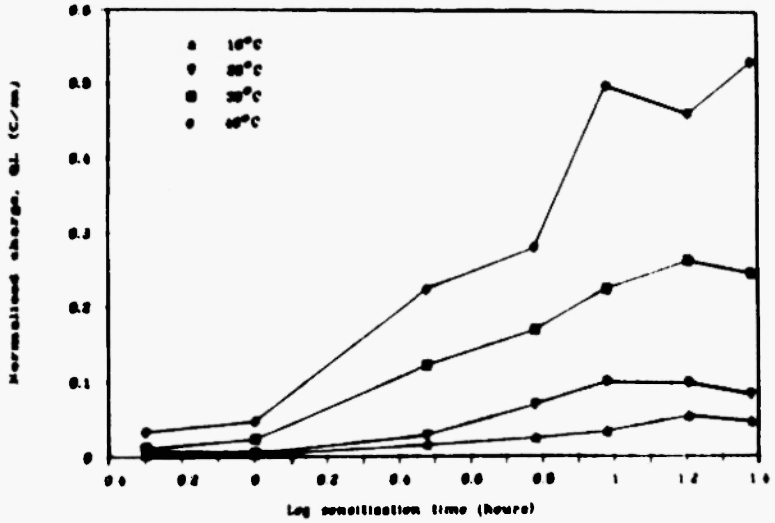

Fig. 8: Effect of sensitization time (at 620°C) and testing temperature on the results of single-loop EPR measurements /32/.

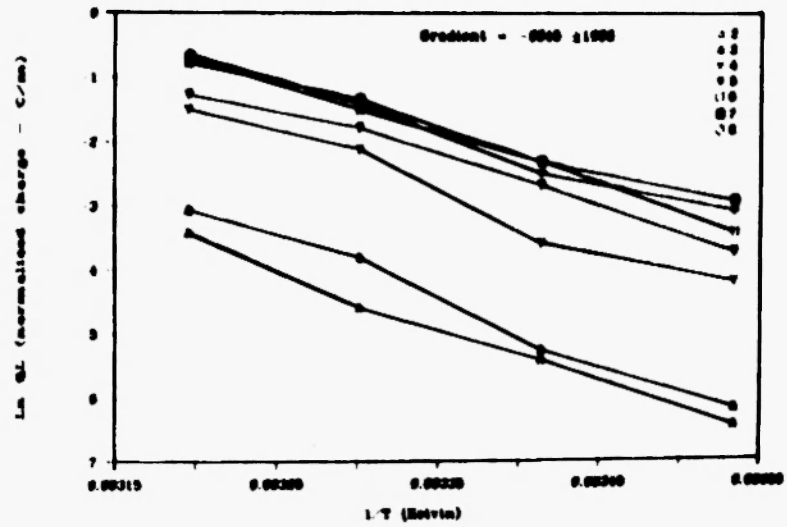

Fig. 9: Arrhenius plot of sensitization data, giving an activation energy for dissolution of 67 ± 9 kJmol^{-1} /32/.

in a nickel-base alloy. Significantly, the width of attacked regions in the EPR test was shown to be temperature-dependent, from about 1.5 μm at 10°C to about 4 μm at 40°C for type 304 SS. This width is considerably higher than the 'width' of Cr-depleted zones, which is of the order of a few 100 Å only. It was suggested by the round robin tests that the conditions during EPR tests are too aggressive and allow dissolution of undepleted regions as well, after dissolution of Cr-depleted regions. However, these conditions are not too aggressive to depassivate the undepleted regions themselves. Therefore, during dissolution of Cr-depleted regions, the solution in the local regions there must be very aggressive to allow spreading of attack to nearby undepleted regions.

Due to these two facts, the round robin study suggested dropping of the 'width' term from the calculation of P_a. Instead, the degree of sensitization was proposed to be expressed as dissolution charge normalized to the grain boundary length and its expression as a Q_L value in Cm^{-1}.

$$Q_L = Q.2\bar{l} / \pi.A \quad (3)$$

Q = dissolution charge
$\bar{l}$ = mean grain boundary intercept length used to evaluate ASTM grain size.
A = specimen area

In order to circumvent the third assumption, in the calculation of GBA, that the grains are circular in shape, Hanninen *et al.* /32/ used this approach:

$$GBA = A \times [5.09544 \times 10^{-3} \exp (0.34696.X)] \quad (4)$$

where $X = 3.2877 - 6.6439 \log_{10} \bar{l}$

$\bar{l}$ = mean linear intercept (mm)

or

$$\bar{l} = \pi/2L_A \quad (5)$$

L_A = length of grain boundary per unit specimen area (mm/mm^2)

$$GBA = L_A.A.W = \pi.A.W/2\bar{l} = 1.57\ A.W/\bar{l} \quad (6)$$

and W is the width of attacked grain boundary regions.

This calculation approach does not assume circular grain shape. The constant of 1.57 in eqn. (6) changes to 1.63 if the assumption of circular grains is accepted, as in eqn. (1).

6.3. Characteristic Parameters of Cr Depletion Zone and EPR Testing

As has been described above, the 'width' attacked in the EPR tests is strongly dependent on the test temperature (i.e. dissolution kinetics) and much more (one hundred times more) than the width of Cr

depletion zones. Therefore, any correlation of the width of depletion zones to the results of EPR tests is not logical. The round robin tests showed that the P_a values are strongly dependent on the length (coverage) of the Cr depletion zones. This is reflected by low P_a values for 'step' or 'dual' structures and high values for 'ditch' structures. However, other studies have shown strong dependence of the 'depth' of Cr depletion zones on the results of EPR tests. This is obvious from the results of desensitization studies (Fig. 7), where /31/ the coverage of grain boundaries is the same (nearly 100%) for the sensitized and desensitized samples; however, the P_a value drops upon desensitization. Although Cr profiling has not been done in these studies, other studies show that, upon desensitization, the width of the depleted zone increases but depth reduces. This is, in fact, indicative of the fact that the minimum percent of Cr in the depletion zone strongly influences the P_a values while width does not affect these results.

This fact was demonstrated by Bruemmer *et al.* /33/ who used STEM studies and their correlation with EPR test results. They showed that for type 304 SS, the samples showing high P_a values have Cr-depleted regions with Cr in the range of 12.5-13.5%. However, they used a volume depletion parameter of the depletion zone to correlate with the EPR degree of sensitization and gave this formula:

$$P_a = 0.42\,(VP) - 5\times10^{-4}\,(VP)^2 + 2\times10^{7}(VP)^3 \qquad (7)$$

where

$VP = (C_{ry} - C_{rm})W_y/2C_{ry}$,

C_{ry} = critical Cr concentration for EPR test, above which depleted regions are not attacked,

C_{rm} = minimum Cr concentration in the depletion zone,

W_y = width of the depleted zone.

The results of a vast number of EPR tests indicate that, for 'step' and 'dual' structures, the results of the EPR test are strongly dependent on the coverage, i.e. the length of grain boundaries covered by Cr depletion zones. The P_a or Q_L value, calculated by eqns. 1 or 3, give a good comparison of this aspect. However, for correlations to IGC or IGSCC, use of parameter Q_L (eqn. 3) or W_L, based on the actual length of grain boundaries attacked, would be more appropriate, as it would be directly indicative of the minimum level of Cr in the Cr-depleted zones.

6.4. Use of Depassivator

Recent investigations have concentrated on the role of an activator or a depassivator in the EPR test /34/. Some investigators reduced the amount of KSCN in the test solution or adopted 3-5N H_2SO_4 solutions. A recent study reported /34/ that the compounds containing S-bearing free electron pairs promoted dissolution of Cr-depleted regions near the grain boundaries of SSs. The S-bearing compounds with the $-CH_3$ radical were more active than those with the $-NH_2$ radical. Among S-bearing free electron pair compounds, CH_3CSNH_2 (thioacetamide) was found to be the most suitable, and the optimum conditions of a revised EPR test were suggested to be: 0.5M H_2SO_4 + 10^{-3}M CH_3CSNH_2, potential scan rate of 100 mV/min, and a vertex potential of 200 mV to 300 mV (SCE).

6.5. Regions Attacked During EPR Tests

As mentioned earlier in sections 6.2 and 6.3, the regions attacked in an EPR test are the Cr-depleted regions and the undepleted regions surrounding the depleted regions. The $M_{23}C_6$ carbides are not attacked as shown in desensitization studies /31/. This was also shown by direct observations of $M_{23}C_6$ particles in the attacked regions when the samples tested by the EPR technique were studied under a TEM /35/.

7. MEASUREMENT OF Cr IN THE DEPLETION ZONE

In order to measure directly the Cr profile in the Cr-depleted regions, Analytical Electron Microscopy (AEM) has been used for stainless steels and nickel-base alloys. On the other hand, some recent reports have mentioned the use of an electrochemical technique to measure the minimum level of Cr in the depletion zones. Both techniques are described below:

7.1. Analytical Electron Microscopy

Quantitative characterization of the amount of Cr depletion adjacent to the intergranular carbide

precipitates, Cr depletion along the segments of grain boundaries that are in between carbides, and measurement of Cr concentration profiles perpendicular to the grain boundary have been reported by many investigators. Use of AEM requires preparation of thin foils of SSs (3 mm diameter discs of about 100 μm thickness) and there are many difficulties associated with the use of AEM for this purpose. These include the following /36/: because of spreading of the electron beam as it travels through the foil, the volume analysed may exceed the size of the chromium depleted zone or the size of the carbide. In such cases, the chromium concentration of the Cr-depleted zone is overestimated and that of the grain boundary carbide underestimated. In order to minimize the effects of the beam broadening and to obtain the optimal spatial resolution, it is necessary to use a small beam size and to analyse a thin region. This results in reduction of the X-rays generated because of the small datum. During this time, the sample of some alloys may also drift, resulting in uncertainty as to the location of the analysed volume. Many studies have used beam sizes of 300 Å for line scan and 100 Å for discrete point X-ray spectra measurement.

Secondly, due to boundary-to-boundary variation in the amount of carbide precipitation and in the level of Cr depletion, a large number of grain boundaries must be measured in order to characterize accurately the Cr concentration of the grain boundaries. This would take a prohibitively long time.

7.2. Quantitative Electrochemical Potentiostatic Test

Due to the difficulties encountered in the AEM studies, Devine *et al.* reported /36/ the use of an electrochemical technique to measure the minimum level of Cr in the depletion zones of stainless steels. The test is based on the facts that in a 0.5M H_2SO_4 + 0.01 M KSCN solution, (a) the active to passive transition occurs over a very narrow range of potential for Fe-10 wt% Ni - Xwt% Cr alloy, (b) the range in potential over which the transition occurs varies markedly with the Cr content of the alloy, and (c) the corrosion rates of the ternary alloys in the active state is 3 to 5 orders of magnitude greater than that in the passive state. The diagram showing the passivation potential of various Fe-10 wt% Ni - Xwt% Cr alloys is shown in Fig. 10 /36/.

The test involves immersion of the sample in a 0.5M H_2SO_4 + 0.01 M KSCN solution (deaerated) at a predetermined potential for 24 hrs. After this the sample is bent through an angle of 90° and the bent surface is examined for intergranular cracks/fissures. The experiment is repeated on different samples at different potentials to establish the minimum potential at which intergranular cracks are not observed. Using Fig. 10, the level of Cr corresponding to this potential is determined and this is the minimum level of Cr in the depletion regions of the sample.

Devine *et al.* /36/ have shown by calculations that the level of Cr thus determined is actually the level of Cr present at a distance of 50 Å from the carbides.

7.3. Magnetic Susceptibility Test

In order to measure the minimum level of Cr in the depleted regions in Alloy 600, magnetic susceptibility testing is the only conventional non-destructive test available /25,26/. This was described in section 4.3.2.

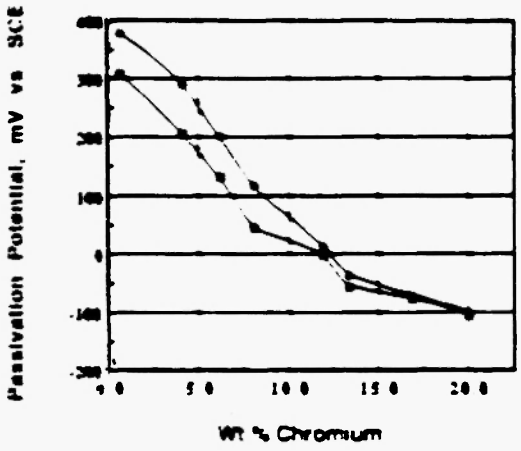

Fig. 10: Influence of chromium on the passivation potential of Fe-10Ni-xCr ternary alloys in 0.5 MH_2SO_4 + 0.01M kSCN. At potentials greater than the solid points the alloy is passive. At potentials less than the open points the alloy is active /36/.

8. DISCUSSION

As is the case with other materials exhibiting 'passivity', Fe-Cr-Ni alloys are also prone to localised forms of corrosion. Though the phenomenon of IGC has been reported for other alloys, e.g. Al alloys, its extent and consequences in Fe-Cr-Ni alloys are enormous. Several theories have been proposed to explain IGC in these alloys, but the Cr depletion theory and the segregation theory (in particular oxidizing media) have been able to explain most of the characteristic features of IGC. Therefore, it is the phenomenon of sensitization, or precipitation of chromium-rich carbide (or nitride in the case of nitrogen-rich alloys) and formations of Cr depletion regions at and adjacent to the grain boundaries that are primarily responsible for IGC.

The effect of major and minor impurity elements on the sensitization characteristics is more or less clearly understood. Using this information, and also thermodynamic analysis, many authors have proposed the use of chemical composition-based parameters to compare the sensitization behaviour of various alloys. However, prediction of the degree of sensitization or susceptibility to IGC using these parameters has not been done except in a few cases. The authors showed /37/ the use of chemical composition-based parameters, $Cr^{effective}$ = %Cr - 0.18 (%Ni)-100(%C) for type 304/304L SSs. It was shown that $Cr^{effective} > 14.0$ ensures the material's resistance to IGC in practice C, A 262, ASTM. Use of a modified heat treatment at 677°C for 20 min was also suggested to arrive at better correlations of Cr^{eff} with IGC rates in practice C, A 262, ASTM.

Barring such an approach to predict IGC behaviour, other test procedures including ASTM standard tests are qualitative in nature (except practice A, A 262, ASTM). The advent of EPR testing provided a non-destructive test which was quantitative as well. However, a number of assumptions made for calculation of the P_a parameter did not allow its direct correlation to the IGC or SCC behaviour of Fe-Cr-Ni alloys. The basic mechanisms of processes occurring during EPR testing are better understood than before, and it is now evident that (a) $M_{23}C_6$ is not attacked during the EPR test, (b) the coverage of grain boundaries by depletion zones is the most important parameter affecting results of EPR tests, (c) for any sensitized grain boundary, the level of Cr in the depletion zone affects the dissolution (reactivation) charge, (d) the width of the depletion zone may not affect the test results at all, as this dimension is affected by dissolution kinetics (a temperature-dependent phenomenon) and the width of attacked regions during the EPR test is always greater than the width of depleted regions by an order of about 100, (e) 'active' inclusions are also etched out during the single-loop test, affecting the results, and (f) prior cold work of the material affects the peak current density for passivation (i_p) and also probably during reactivation (i_r), allowing only use of the ratio C_r/C_a to correlate well with the results of modified practice E, A 262, ASTM.

Though the use of EPR testing is popular for type 304/304L SSs, it is not as common for type 316/316L or duplex SSs and nickel-base alloys. The main reason for this is the lack of agreement on the optimum conditions and also the lack of correlations between the results of EPR tests and the susceptibility to IGC or SCC for these materials. As the mechanisms of processes taking place during the EPR tests become clear for type 304/304L SSs, basic understanding of these mechanisms in other alloys will also follow, thus promoting the use of the EPR test and its further development for other Fe-Cr-Ni alloys as well.

Other electrochemical methods, e.g., constant potential etching and quantitative electrochemical potentiostatic tests, also detect sensitization of Fe-Cr-Ni alloys. The constant potential etching technique in $HClO_4$ + HCl solutions for high-alloy SSs has been shown to be sensitive to materials with low to medium levels of sensitization. The sensitivity is reported to be higher than that observed in the modified strauss test. The other technique, a quantitative electrochemical potentiostatic technique, has not been used for detection of sensitization as such. However, for prediction of comparative susceptibility to IGC, this technique is very valuable. It has been shown by authors that SSs with 'step' or 'dual' structures do not undergo IGC in practice C, A 262, ASTM. However, materials with a 'ditch' structure would have different susceptibility to IGC depending upon the minimum level of Cr in their depletion zones. Therefore, for materials with a 'ditch' structure, this quantitative electrochemical potentiostatic technique can be used to determine the minimum level of Cr in the depletion zones. If this minimum

level of Cr is more than 12-13%, the material would not undergo IGC. If this level of Cr is less in one material, it would show higher intergranular corrosion rate than the material having higher levels of Cr in its depletion zones. This technique is easier to carry out and a number of samples can be tested simultaneously to arrive at the minimum level of Cr in the depletion zones, thus avoiding the use of the more tedious technique of AEM to do the same.

For nickel-base alloys, Inconel 800/.600, the use of the non-destructive test based on magnetic susceptibility holds promise. Detection of sensitization and even the determination of a minimum level of Cr in the depletion zones allows prediction of their degree of sensitization/susceptibility to IGC. Other non-destructive tests have not been successful in detecting sensitization in SSs.

9. CONCLUSIONS

The Fe-Cr-Ni alloys are commonly used in high-temperature applications. However, exposure to the temperature range of 475-800°C (during either service or fabrication) induces sensitization and may render them prone to intergranular corrosion (IGC). The following points emerge from the large amount of research work carried out regarding sensitization, IGC and their detection in Fe-Cr-Ni alloys:

(1) The Cr depletion theory explains the mechanism of sensitized alloys, whereas the segregation theory explains the IGC of non-sensitized alloys in oxidizing environments;
(2) In general, higher levels of Cr, Mo and N and lower levels of Ni and C are beneficial in reducing sensitization, and the effect of individual alloy/impurity addition on the precipitation of $M_{23}C_6$/IGC is well understood;
(3) The commonly used ASTM standard methods to assess a material's susceptibility to IGC are time-consuming and destructive in nature, and the chemical composition-based parameter [$Cr^{effective}$ = %Cr-0.18 (%Ni)-100 (%C)] has been correlated to the results of practices C and E, A 262, ASTM, and this can be used to predict the susceptibility of type 304/304L SSs to IGC, without actually resorting to the lengthy ASTM practices.
(4) The EPR tests are now commonly used to evaluate the degree of sensitization (DOS) of Fe-Cr-Ni alloys. However, the P_a values are sensitive to distinguish materials with low DOS and saturate for materials with high DOS. Therefore, correlations of the results of EPR tests with the results of IGC tests for materials with 'ditch' structures are not possible.
(5) The characterization of Cr depletion zones having three parameters, length (coverage), width and depth (i.e. minimum level of Cr in the depletion zones) has added new dimensions to the phenomenon of sensitization, IGC and its detection.
(6) The results of EPR tests are most sensitive to the coverage and then to the depth of Cr depletion zones, and mechanisms of processes occurring during EPR tests are now better understood.
(7) In addition to sensitization, the effect of other variables, e.g., prior cold work, presence of inclusions and desensitization on the results of EPR tests, is clearly understood.
(8) The use of a chemical composition-based parameter, $Cr^{effective}$, along with microstructure classification as per practice A, A 262, ASTM leaves fewer materials with 'ditch' structures for checking their susceptibility to IGC. This can also be done without actually carrying out the lengthy A 262 tests, by electrochemical tests to assess the minimum level of Cr in the Cr depletion zones. For alloy 600, magnetic susceptibility tests serve this purpose.

The focus for future work should be on (a) development of commonly acceptable conditions for EPR tests for various Fe-Cr-Ni alloys so as to include these in standards, (b) agreement on acceptance limits for various alloys for ASTM tests, and (c) development of NDT techniques to detect sensitization in SSs.

10. ACKNOWLEDGEMENTS

The authors are grateful to Dr. C.K. Gupta, Director, Materials Group, B.A.R.C., for his encouragement and permission to publish the paper. They are also thankful to Dr. S. Banerjee, Head,

Metallurgy Division, for his interest and suggestions during the preparation of the manuscript.

11. REFERENCES

1. A.J. Sedricks, *Corrosion of Stainless Steels*, John Wiley & Sons, New York, 1979.
2. J.D. Redmond and K.H. Miska, *The Chemical Engineering Guide to Corrosion Control in the Process Industries*, R.W. Greene (ed.), McGraw-Hill Publications Co., New York, 1986; p. 168.
3. R.L. Cowan II and C.S. Tedmon Jr., *Advances in Corrosion Science and Technology*, Vol. 3, M.G. Fontana and R.W. Staehle (eds.), Plenum Press, New York, 1973; p. 293.
4. E.C. Bain, R.H. Aborn and J.J.B. Rutherford, *Trans. Am. Steel Treating Soc.*, **21**, 481 (1933).
5. H.D. Solomon and T.M. Devine, Report No. 78CRDO85, General Electric, May, 1973.
6. J.A. Collins and M.L. Monack, *Mater. Perf*, **12**, 11 (1973).
7. V. Cihal, *Intergranular Corrosion of Stainless Alloys*, SNTL, Prague, 1967.
8. E.L. Hall and C.L. Briant, *Metall. Trans.*, **15A**, 793 (1984).
9. S.M. Bruemmer and L.A. Charlott, *Scripta Metall.*, **20**, 1019 (1986).
10. V. Cihal, *Prot. Met.*, **4**, 563 (1968).
11. C.L. Briant, R.A. Mulford and E.L. Hall, *Corrosion*, **38**, 468 91982).
12. R.S. Dutta, P.K. De and H.S. Gadiyar, *Corr. Sci.*, **34**, 51 (1993).
13. M.A. Streitcher, *Intergranular Corrosion of Stainless Alloys*, ASTM STP-656, ASTM, Philadelphia, 1978; p. 3.
14. H. Hannin, *Int. Met. Reviews*, **24**, 85 (1979).
15. V. Cihal, A. Desestret, M. Froment and G.H. Wagner, *5th European Corrosion Congress*, Paris, 24-28 Sept., 1973.
16. M. Prazak, *Corrosion*, 19(3), 75 (1963).
17. A.P. Majidi and M.A. Streitcher, *Corrosion*, **40**, 393 (1984).
18. C.S. Tedmon and D.A. Vermilyea, *Corrosion*, **27**, 376 (1971).
19. M. Akashi, T. Kawamoto, F. Umemura and Boshoku Gijutsu, *Corrosion Engg.*, **29**, 163 (1980).
20. A.P. Majidi and M.A. Streitcher, *Corrosion*, **40**, 584 (1984).
21. P.R. Singh and H.S. Gadiyar, *Proceedings of Workshop on Non-Destructive Evaluation in Corrosion (NECOR)*, IGCAR, Akkam, Jan. 29-31, 1992; iii.3, p. 1.
22. M.K. Ahn, H.S. Kwon and J.H. Lee, *Corrosion*, **6**, 441 (1995).
23. J.P. Sydow, D.L. Reichert and G.E. Stoner, *Mat. Perf.*, **30**(1), 68 (1991).
24. R. Qvafort, *Corrosion*, **51**, 463 (1995).
25. M. Kowaka, H. Nagano, T. Kudo, Y. Okada *et al.*, *Nuclear Technology*, **55**, 340 (1981).
26. A. Borello and A. Mignone, *Brit. Corr. J.*, **17**, 176 (1982).
27. B.K. Shah, M.Tech. Dissertation, IIT, Bombay, 1984.
28. V. Kain, S.S. Chouthai and H.S. Gadiyar, *ASTM J. Testing & Evaluation*, **19**, 321 (1991).
29. A. Bose and P.K. De, *Corrosion*, **43**, 624 (1987).
30. V. Kain, S.S. Chouthai and H.S. Gadiyar, *Brit. Corr. J.*, **27**, 59 (1992).
31. K.N. Adhe, V. Kain, S.S. Chouthai and H.S. Gadiyar, *J. Electrochem. Soc. (India)*, **28**, 139 (1990).
32. H. Hanninen, Final Report of the NKA Project-MAT 530, VTT, Finland, September, 1989.
33. S.M. Bruemmer, L.A. Charlott and B.W. Arey, *Corrosion*, **44**, 328 (1988).
34. Z. Fang, L. Zhang, Y.S. Wu, J.Q. Li, D.B. Sun, C. Jiang and Z.M. Cui, *Corrosion*, **51**, 124 (1995).
35. I. Aho-Mantila, P. Aaltonen and H. Hanninen, Technical Research Centre of Finland, VTT-MET-B 26, Espoo, Finland, 1981.
36. T.M. Devine, *Corr. Sci.*, **30**, 135 (1990).
37. V. Kain, R.C. Prasad, P.K. De and H.S. Gadiyar, *ASTM J. Testing & Evaluation*, **23**, 50 (1995).